Available online at www.sciencedirect.com
ScienceDirect
Acta Materialia 54 (2006) 4385–4391
Acta MATERIALIA
www.actamat-journals.com

The role of antiphase boundaries in the kinetic process of the $L1_2 \rightarrow D0_{22}$ structural change of an $Ni_3Al_{0.45}V_{0.50}$ alloy

Makoto Tanimura [a,*], Yasumasa Koyama [b]

[a] *Research Department, NISSAN ARC LTD., Yokosuka, Kanagawa 237-0061, Japan*
[b] *Kagami Memorial Laboratory for Materials Science and Technology and Department of Materials Science and Engineering, Waseda University, Shinjuku, Tokyo 169-8555, Japan*

Received 27 March 2006; received in revised form 15 May 2006; accepted 19 May 2006
Available online 4 August 2006

Abstract

The influence of antiphase boundaries (APBs) on the kinetic process of the $L1_2 \rightarrow D0_{22}$ structural change in an $Ni_3Al_{0.45}V_{0.50}$ alloy has been investigated by transmission electron microscopy. The structural change includes two kinetic factors, i.e., the periodic introduction of antiphase-shifted planes (APSPs) in the $L1_2$ structure and V diffusion in the $L1_2$ matrix. Our results revealed that APB migration was accompanied by V diffusion as if to sweep the V atoms out of the antiphase domains (APDs). It was also found that the APBs served as the nucleation sites of the $D0_{22}$ regions, because the combination of the migrated APBs produced the APSPs in the $L1_2$ structure. On this basis, it is proposed that the APBs bring together the two kinetic factors in the process of the $L1_2 \rightarrow D0_{22}$ structural change, the physical origin of which is the variation in the charge density distribution of the APDs due to APB migration.

Keywords: Isothermal heat treatments; Transmission electron microscopy; Nickel alloys; Phase transformation kinetics; Diffusion in ordered structures

1. Introduction

The topology of the atomic arrangement in crystal structures has often attracted researchers' interest. An antiphase boundary (APB), which is frequently observed in ordered structures in alloys and ionic crystals, is an example of a topological defect in a crystal structure and plays a crucial role in the formation of a "topological structure". For example, a long-period superstructure (LPS) in alloys is formed when APBs are introduced with a certain period in a normal structure. The formation of LPSs has been actually found in some alloys such as Au–Cu, 2H–$TaSe_2$, Ag–Mg, and Cu–Al [1–5]. So far, the LPS has been explained as a topological modulation of the normal structure, the physical origin of the modulated wave often being a charge density wave (a CDW). In this case, the LPSs are stabilized as a response to the appearance of the CDWs. The period of a CDW is determined by the radius of the flattened portions of the Fermi surface (the magnitude of the $\mathbf{k_f}$ vector in reciprocal space) and varies from incommensurate to commensurate with a decrease in temperature [1,2,6–9]. On this basis, incommensurate–commensurate (or normal) structure transitions of the LPSs have been extensively studied experimentally and theoretically from the viewpoint of the topological change [1–13].

With regard to topological structures, the relation between the face-centred cubic (fcc)-based $L1_2$ and $D0_{22}$ ordered structures with an ideal composition of A_3B is also worthy of attention. As shown in Fig. 1 the $D0_{22}$ structure is formed by the antiphase atomic displacement along the $[1\,1\,0]_f$ direction on every other $(0\,0\,1)_f$ plane in the $L1_2$ structure, where the subscript f denotes the fcc notation. That is, the $D0_{22}$ "topological structure" is characterized by the periodic introduction of antiphase-shifted planes (APSPs) in the $L1_2$ "normal structure". It is thus understood that the change between the $L1_2$ and the $D0_{22}$ structures is described by the topological change due to the introduction or annihilation of the APSPs.

* Corresponding author. Tel.: +81 468 67 5282; fax: +81 468 66 5814.
E-mail address: tanimura@nissan-arc.co.jp (M. Tanimura).

1359-6454/$30.00
doi:10.1016/j.actamat.2006.05.031

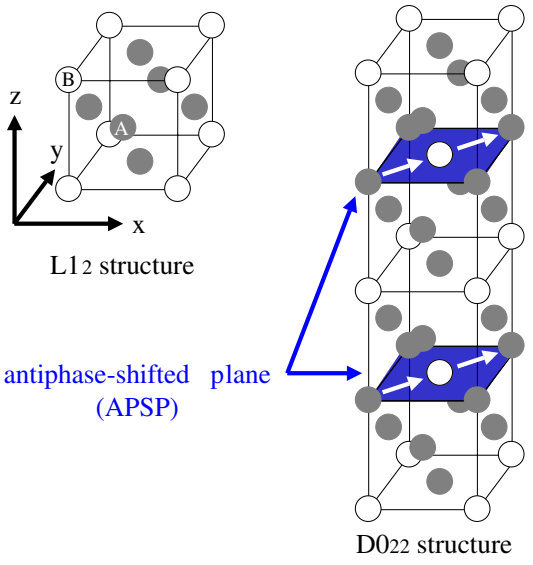

Fig. 1. $L1_2$ and $D0_{22}$ structures. White and black circles in the $L1_2$ structure represent A- and B-site atoms, respectively. The $D0_{22}$ structure is formed by the periodic introduction of an APSP on every other (0 0 1) plane of the $L1_2$ structure. Note that APSPs are characterized by the antisite atomic displacement along the [1 1 0] direction.

The stability of the $L1_2$ and $D0_{22}$ structures has been studied with respect to the number of valence electrons per atom (e/a) [14–16]. Specifically, the $D0_{22}$ structure is stable when e/a is larger than 8.60, while the $L1_2$ structure appears when e/a is smaller than 8.60. Because the e/a variation generally results from changes in alloy composition, this e/a classification rule indicates that the $L1_2 \leftrightarrow D0_{22}$ structural changes basically arise from a variation in chemical composition. Thus, the structural changes include two kinetic factors, i.e., atomic diffusion and topological change, which is a crucial difference from the case of the incommensurate–commensurate transition.

The $L1_2 \leftrightarrow D0_{22}$ structural changes normally occur in a ternary alloy system with a specific combination of the $L1_2$-stabilized and $D0_{22}$-stabilized alloys. A prominent example of such a combination is that of Ni_3Al ($L1_2$) and Ni_3V ($D0_{22}$) alloys, which constitute a pseudobinary $Ni_3Al_{1-x}V_x$ alloy system [17]. We have investigated the kinetic process of the $Ni_3Al_{1-x}V_x$ (supersaturated $L1_2$) $\rightarrow Ni_3Al$ ($L1_2$) + Ni_3V ($D0_{22}$) phase separation of $Ni_3Al_{1-x}V_x$ alloys with $0.40 \leqslant x \leqslant 0.60$ under isothermal conditions [18–20]. It should be noted that the phase separation is characterized by $D0_{22}$ precipitation in the supersaturated $L1_2$ matrix (the occurrence of the $L1_2 \rightarrow D0_{22}$ structural change), where long-range V diffusion in the $L1_2$ matrix is dominant. It has been found, however, that a blocking effect of V diffusion appears in the $L1_2$ matrix with few APBs and stagnates $D0_{22}$ precipitation in the alloys with $0.40 < x < 0.55$, resulting in the formation of a single $L1_2$ final state [20]. The stagnation stems from the independence of V diffusion on the topological change during the $L1_2 \rightarrow D0_{22}$ structural change.

In the study reported here, we focused on the kinetic process of the $L1_2 \rightarrow D0_{22}$ structural change of the $Ni_3Al_{0.45}V_{0.50}$ alloy from the viewpoint of the role of APBs. The alloy composition used differed slightly from the ideal A_3B composition in order to introduce numerous APBs in the supersaturated $L1_2$ matrix.

2. Experimental

An ingot of the $Ni_3Al_{0.45}V_{0.50}$ alloy was made using an Ar arc melting technique. The chemical composition of the ingot was confirmed by inductively coupled plasma spectroscopy (ICP). In reference to the phase diagram [17], the samples cut from the ingot were homogenized at 1623 K (fcc region) for 24 h, followed by quenching in ice water. As is shown later, the quenched samples consisted of the $L1_2$ single state with numerous APBs. In order to induce the $L1_2 \rightarrow D0_{22}$ structural change, the quenched samples were kept at 1173 K ($L1_2 + D0_{22}$ region) for up to 500 h and then quenched in ice water again.

All of the specimens for transmission electron microscopy observation were prepared from the respective samples by mechanical polishing and ion thinning methods. The electron diffraction patterns and the microstructures of the specimens were observed at room temperature using an H-800 transmission electron microscope operated at 200 keV. Energy dispersive X-ray (EDX) spectra and EDX mapping diagrams were obtained using a TECNAI G^2 F20 scanning transmission electron microscope (200 keV) with an electron probe of about 1 nm in diameter. The chemical compositions of the $L1_2$ matrix and the $D0_{22}$ precipitates that appeared in the respective samples were quantified using the Ni Kα, Al Kα, and V Kα lines. For statistical reliability in the EDX analysis, photon counts of more than 200,000 were detected at each analysed point and a quantitative accuracy of about $x = \pm 0.02$ was determined on the basis of a comparison between the average EDX values and the ICP values of the quenched samples.

3. Results

First of all, we will give an explanation of the microstructure change accompanied by the $L1_2 \rightarrow D0_{22}$ structural change. Fig. 2a and b shows a typical microstructure, together with an electron diffraction pattern, obtained from the quenched alloy. The electron incidence is parallel to the [0 0 1] direction. It should be mentioned here that, for simplicity, all of the Miller indices are denoted in terms of the fcc notation. The appearance of the forbidden spots (e.g., 1 0 0-type spots) in the diffraction pattern in Fig. 2a is indicative of the occurrence of $L1_2$ ordering during the quenching process. The bright-field image in Fig. 2a displays the features of the microstructure in one crystal grain. The average size of the crystal grains is as large 100 μm because of the long homogenization time of 24 h. In the image, no characteristic contrast, except for some dislocations, can be observed in the grain. A corresponding dark-field image taken using a 1 0 0 forbidden spot is shown in Fig. 2b. The